Engineering Arbitrary Hamiltonians in Phase Space

Lingzhen Guo[1,2,*] and Vittorio Peano[2]

[1]Center for Joint Quantum Studies and Department of Physics, School of Science, Tianjin University, Tianjin 300072, China
[2]Max Planck Institute for the Science of Light, Staudtstrasse 2, 91058 Erlangen, Germany

(Received 9 February 2023; revised 27 June 2023; accepted 27 November 2023; published 11 January 2024)

We introduce a general method to engineer arbitrary Hamiltonians in the Floquet phase space of a periodically driven oscillator, based on the noncommutative Fourier transformation technique. We establish the relationship between an arbitrary target Floquet Hamiltonian in phase space and the periodic driving potential in real space. We obtain analytical expressions for the driving potentials in real space that can generate novel Hamiltonians in phase space, e.g., rotational lattices and sharp-boundary wells. Our protocol can be realized in a range of experimental platforms for nonclassical state generation and bosonic quantum computation.

DOI: 10.1103/PhysRevLett.132.023602

Introduction.—Generation of nonclassical bosonic states [1–3], e.g., squeezed lights, Fock states, and Schrödinger's cat states, is important not only for fundamental studies of quantum mechanics but also for applications in quantum technologies [2,4–6]. For example, bosonic states with discrete translational or rotational symmetries in phase space [7–14] have been proposed to encode quantum information [15–20], paving the way for hardware-efficient quantum error correction [21–24]. Bosonic code states can be prepared and stabilized against dissipation via, e.g., interleaved selective number-dependent arbitrary phase (SNAP) and displacement gates [25–27]. A series of recent works [28–31] have pointed to an alternative passive control approach based on Hamiltonian engineering that can be leveraged to facilitate fault-tolerant operations, e.g., by suppressing phase flip errors [28], suppressing dynamically the coupling to the environment [30], and accelerating state preparation of code words [31].

Another area of interest for Hamiltonian engineering is topology. Because of the noncommutative nature of phase space, a quantum particle moving on a closed phase-space loop acquires a geometric phase analogous to the Aharonov-Bohm phase for particles in magnetic fields. As a consequence, a gapped lattice Hamiltonian in phase space can support nontrivial Chern numbers [16,32–40]. This is an appealing feature because in a system with a physical boundary, it would lead to topologically robust edge transport. While it has been shown how to generate arbitrary lattice potentials in phase space [41], so far it is unclear how to combine such a potential with a sharp phase-space confinement.

It is well known that the stroboscopic dynamics of any time-periodic system can be described in terms of a time-independent Floquet Hamiltonian $\hat{H}_F$ defined via [42–44]

$$\exp\left(\frac{1}{i\lambda}\hat{H}_F T\right) \equiv \hat{U}(T,0) = \mathcal{T}\exp\left[\frac{1}{i\lambda}\int_0^T \hat{H}(t)dt\right]. \quad (1)$$

Here, $\hat{U}(T,0)$ is the time-evolution operator with T the time period of the system's time-dependent Hamiltonian $\hat{H}(t)$. In addition, λ is an effective dimensionless Planck constant, and $\mathcal{T}$ is the time-ordering operator. Except for very few models, it is impossible to obtain a closed form of the Floquet Hamiltonian $\hat{H}_F$ from $\hat{H}(t)$. Instead, one often evaluates $\hat{H}_F$ relying on a high-frequency expansion [45,46], e.g., Magnus expansion theory [47,48], van Vleck degenerate perturbation theory [42], and Brillouin-Wigner perturbation theory [49]. In this work, we focus on the inverse problem, that is, to find the time-dependent Hamiltonian $\hat{H}(t)$ that synthetizes a target Floquet Hamiltonian $\hat{H}_F^{(T)}$. This is the realm of Floquet engineering which is a very developed and active field [39,43,50–52]. Most of the work so far has focused on implementing specific Floquet Hamiltonians of interest. However, a systematic constructive method to solve the inverse Floquet problem for a single quantum particle is still missing. In this work, we provide such a method.

Model and goal.—As a starting point, we consider a periodically driven oscillator with lab-frame Hamiltonian

$$\hat{\mathcal{H}}(t) = \frac{\omega_0}{2}(\hat{p}^2 + \hat{x}^2) + \beta V(\hat{x}, t). \quad (2)$$

Here, ω_0 is the oscillator natural frequency, β is the amplitude of the nonlinear driving potential $V(\hat{x},t)$ which has time-period T_d and might contain also static terms. In order to introduce an effective dimensionless Planck constant λ [53–55], the position $\hat{x}$, the momentum $\hat{p}$, and $\hat{\mathcal{H}}(t)$ have been rescaled such that $[\hat{x},\hat{p}]=i\lambda$ and at the same time the Schrödinger equation reads $i\lambda\dot{\psi}=\hat{\mathcal{H}}(t)\psi$. Parameter λ measures the quantumness of our system and $\lambda\to 0$ corresponds to the classical limit.

The Floquet Hamiltonian to be designed is defined via $\hat{O}(t)=\exp[i\hat{a}^\dagger\hat{a}t]$ with time period $T=2\pi/\omega_0$, where $\hat{a}=(\hat{x}+i\hat{p})/\sqrt{2\lambda}$ is the annihilation operator. In other words, $\hat{H}(t)$ in Eq. (1) is the rotating-frame Hamiltonian given by $\hat{H}(t)=\hat{O}(t)\hat{\mathcal{H}}(t)\hat{O}^\dagger(t)+i\lambda\dot{\hat{O}}(t)\hat{O}^\dagger(t)$, which in our case reads

$$\hat{H}(t)=\beta V[\hat{x}\cos(\omega_0 t)+\hat{p}\sin(\omega_0 t),t]. \tag{3}$$

We enforce the time periodicity, $\hat{H}(t)=\hat{H}(t+T)$, by setting $T=qT_d$ with $q\in\mathbb{N}\geq 1$, corresponding to a q-photon resonance. Any detuning from the multiphoton resonance is formally incorporated in the driving potential $V(x,t)$. For weak nonlinearity, $\beta\ll\omega_0$, the evolution in the rotating frame is slow. Thus, we are in the realm of application of the Floquet high-frequency expansions, here, with the small parameter β/ω_0. This allows us to approximate the Floquet Hamiltonian with the leading order of the Floquet-Magnus expansion corresponding to the rotating wave approximation (RWA),

$$\lim_{\omega_0/\beta\to\infty}\hat{H}_F(\hat{x},\hat{p})=\frac{1}{T}\int_0^T dt\,\hat{H}(t). \tag{4}$$

Our goal is to engineer an arbitrary target Floquet Hamiltonian $\hat{H}_F^{(T)}$ in phase space by properly designing the driving potential $V(x,t)$ in real space. Up to leading order (RWA) we, thus, require that the right-hand side of Eq. (4) coincides with the target Hamiltonian $\hat{H}_F^{(T)}$. The ensuing solution becomes exact in the high-frequency limit $\omega_0/\beta\to\infty$.

NcFT technique.—As a preliminary step towards deriving a suitable driving potential $V(x,t)$, we introduce a useful decomposition of the target Hamiltonian $\hat{H}_F^{(T)}$ in the form of a noncommutative Fourier transformation (NcFT). This can be viewed as a variant of quantum distribution theory [56]. We wish to decompose the target Hamiltonian $\hat{H}_F^{(T)}$ as a sum of plane-wave operators

$$\hat{H}_F^{(T)}=\frac{\beta}{2\pi}\iint dk_x dk_p\, f_T(k_x,k_p)e^{i(k_x\hat{x}+k_p\hat{p})}. \tag{5}$$

It can be shown that the Fourier coefficients $f_T(k_x,k_p)$ are given by the inverse transformation (see Supplemental Material (SM) Sec. I [57])

$$f_T(k_x,k_p)=\frac{e^{\frac{\lambda}{4}(k_x^2+k_p^2)}}{2\pi\beta}\iint dxdp H_Q^{(T)}(x,p)e^{-i(k_x x+k_p p)}, \tag{6}$$

where the phase-space function $H_Q^{(T)}(x,p)$ is the equivalent of the Husimi Q function, here, for a Hamiltonian instead of the density operator. We remind that the Q function of an operator evaluated at a phase space point (x,p) is simply its expectation value in the corresponding coherent state, $H_Q^{(T)}(x,p)=\langle\alpha|\hat{H}_F^{(T)}|\alpha\rangle$ with $\hat{a}|\alpha\rangle=\alpha|\alpha\rangle$ and $\alpha=(x+ip)/\sqrt{2\lambda}$. The latter mean value can be calculated by normal ordering the target Hamiltonian $\hat{H}_F^{(T)}(\hat{a}^\dagger,\hat{a})$. We point out three important features of the Hamiltonian Q function: (i) for fixed λ, the mapping between Floquet Hamiltonians and Q functions is one to one; (ii) the Hamiltonian Q function has the same phase-space symmetries as the corresponding Floquet Hamiltonian, and (iii) a well-defined classical limit $H_F^{(T)}(x,p)\equiv\lim_{\lambda\to 0}H_Q^{(T)}(x,p)$ (see SM Secs. II and IX [57]).

Designing driving potential.—The driving potential $V(x,t)$ that generates the target Floquet Hamiltonian $H_F^{(T)}(\hat{x},\hat{p})$ can be readily obtained from its Fourier coefficient $f_T(k_x,k_p)$. We can formally write the solution as a superposition of cosinusoidal potentials

$$V(x,t)=\int_0^{+\infty}A(k,\omega_0 t)\cos[kx+\phi(k,\omega_0 t)]dk \tag{7}$$

with time-varying amplitudes $A(k,\tau)$ and phases $\phi(k,\tau)$ determined from the Fourier coefficients in polar coordinates ($k_x=k\cos\tau$, $k_p=k\sin\tau$)

$$A=k|f_T(k\cos\tau,k\sin\tau)|,\quad \phi=\mathrm{Arg}f_T(k\cos\tau,k\sin\tau). \tag{8}$$

This solution can be readily verified by plugging it into Eqs. (3) and (4), and changing the integration variables back to Cartesian coordinates to arrive at Eq. (5) (see SM Sec. III [57]). In the remainder of this Letter, we demonstrate the flexibility of our method by calculating the potential $V(x,t)$ for a range of interesting Floquet Hamiltonians. In passing, we will also highlight more general features of our solution and comment on certain associated subtleties.

Example I: Rotational lattice.—We now apply our method to engineer a particularly interesting Floquet Hamiltonian with q-fold symmetry in phase space

$$\hat{H}_F^{(T)}=\beta[(\hat{x}-i\hat{p})^q-1][(\hat{x}+i\hat{p})^q-1]. \tag{9}$$

The discrete rotational symmetry can be described by $\hat{R}(2\pi/q)\hat{H}_F^{(T)}\hat{R}^\dagger(2\pi/q)=\hat{H}_F^{(T)}$, where $\hat{R}(\theta)=\exp(i\hat{a}^\dagger\hat{a}\theta)$ is a phase-space rotation by an angle θ [20,37]. This Hamiltonian supports q global minima, cf. the Q function in Fig. 1 (left) for $q=6$. Here, we have rescaled the

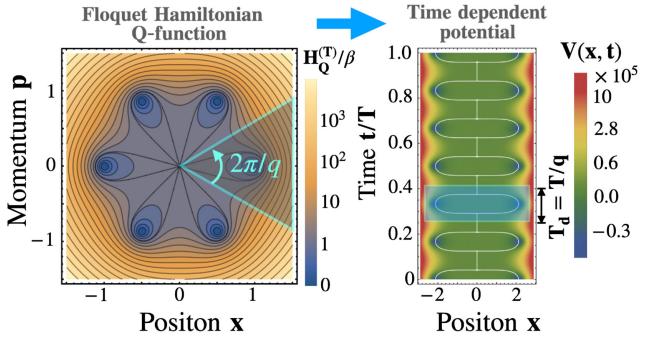

FIG. 1. Rotational lattice Hamiltonian in phase space. (Left) Q function $H_Q^{(T)}(x,p)$ of target Floquet Hamiltonian Eq. (9); (Right) the engineered real-space potential $V(x,t)$ for parameters $q=6$ and $\lambda=0.01$. The white contours indicate the minima of the instantaneous real-space potential.

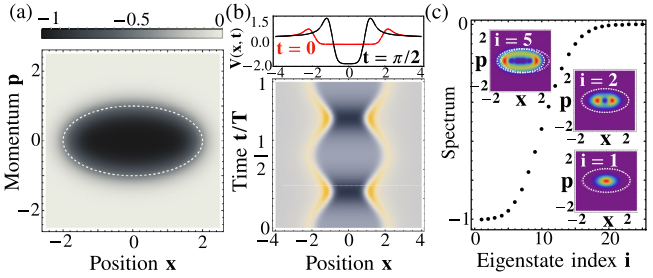

FIG. 2. Elliptical well in phase space. (a) Hamiltonian Q function $H_Q^{(T)}(x,p)/\beta$ with long axis $a=2$, short axis $b=1$, $\lambda=0.1$, and convolution factor $\sigma=\sqrt{\lambda}$. (b) Designed driving potential $V(x,t)$ in one Floquet period (lower) and at instants $t=0$, $t=\pi/2$ (upper). (c) Energy spectrum and Husimi Q functions of ground state ($i=1$), first excited state ($i=2$), fourth ($i=5$) excited eigenstates. The dashed circles in (a) and (c) indicate the boundary of the elliptical well.

phase-space coordinates such that the q global minima fulfill $|x+ip|=1$ corresponding to different classical solutions. Remarkably, quantum fluctuations do not introduce any tunneling between these solutions as the corresponding coherent states $|\alpha_m\rangle=|e^{im(2\pi/q)}/\sqrt{2\lambda}\rangle$ with $m=0,1,\ldots,q-1$ are exact zero-energy eigenstates. In other words, the ground state manifold is q-dimensional space spanned by q q-legged cat states.

Note that since the Hamiltonian Q function is a polynomial, its Fourier transformation Eq. (6) is divergent. To solve this problem, we renormalize the divergence introducing the bounded Hamiltonian $\hat{H}_{F\gamma}^{(T)}=U_\gamma\hat{H}_F^{(T)}U_\gamma$ with $U_\gamma\equiv e^{-\gamma\hat{a}^\dagger\hat{a}}$. Obviously, $\lim_{\gamma\to0}\hat{H}_{F\gamma}^{(T)}=\hat{H}_F^{(T)}$. We can calculate analytically $f_T(k_x,k_p)$ and $V(x,t)$ for $\hat{H}_{F\gamma}^{(T)}$ for any arbitrary positive integer q and $\gamma>0$. This allows us to arrive at a closed expression for the driving potential in the limit $\gamma\to0$ (see SM Sec. IV [57])

$$V(x,t)=\sum_{m=1}^{q}B_{q,m}\lambda^{q-m}x^{2m}-C_q\cos(q\omega_0 t)x^q, \qquad (10)$$

with $B_{q,m}=[(2^m q!)^2(-1)^{q+m}/(2m)!(q-m)!]$ and $C_q=\{2\sqrt{\pi}q!/\Gamma[(2q+3-(-1)^q)/4]\}$. We note that for $q=2$ we recover a well-known result: Eq. (10) corresponds to a parametrically driven Duffing oscillator [53,54,94,95]. We further note that the driving period is $T_d=T/q$ which directly follows from the q-fold rotational symmetry of the Floquet Hamiltonian.

Realizing Hamiltonian (9) is appealing in view of quantum computation because weak photon decay, with rate $\kappa\ll2\beta q^2$, steers the oscillator towards its ground state manifold containing code and error spaces of cat code [8], see Ref. [28] for $q=2$ and SM for the general case [57]. In the SM Sec. V [57], we numerically verify the quality of the weak dissipation and rotating wave approximation for realistic parameters.

Example II: Sharp-boundary well.—Next, we demonstrate that our method allows us to engineer wells with a sharp boundary in phase space. For concreteness we choose an elliptical shape, i.e., $H_Q^{(T)}(x,p)=-\beta$ inside the white dashed line in Fig. 2(a) and $H_Q^{(T)}=0$ otherwise. In the classical limit $\lambda\to0$, our method allows us to find a closed-form solution for $V(x,t)$ (see SM Sec. VII [57]). However, our solution is divergent at two time-dependent positions. In addition, it does not directly apply to the quantum regime, $\lambda\neq0$, because the dependence of $V(x,t)$ on λ is not analytical. This is due to the exponential factor in Eq. (6) leading to divergent NcFT coefficients $f_T(k_x,k_p)$ in the limit of large wave vectors, $k_x^2+k_p^2\to\infty$, for any $\lambda\neq0$. We remove these unphysical features by smoothing out the target Floquet Hamiltonian by applying a convolution with a Gaussian kernel with standard deviation σ, cf. Fig. 2(a). For σ above a threshold, $\sigma>\sqrt{\lambda/2}$, the NcFT coefficient $f_T(k_x,k_p)$ becomes integrable and, thus, leads to a smooth solution for $V(x,t)$, cf. Fig. 2(b) and the closed expression in the SM Sec. VII [57]. This implies that we can implement a potential step that is arbitrarily sharp compared to the typical dimensions of phase-space well, but should remain smooth on the scale of the oscillator quantum fluctuations. Note that Floquet Hamiltonians with sharper boundaries ($\sigma<\sqrt{\lambda/2}$) are well defined but cannot be realized using our method (see SM Secs. II and VII [57]). The spectrum and first few eigenmodes are also shown in Fig. 2(c). The latter are squeezed non-Gaussian states.

Example III: Moiré superlattice.—In Ref. [41], we have shown how to synthesize arbitrary lattices in phase space. We can use our method to combine a lattice potential with a sharp confinement realizing a finite-size lattice. For concreteness we focus on a Moiré superlattice, cf. Fig. 3(a). This is the phase-space equivalent of the 2D potential for electrons in twisted graphene [96–99]. The Moiré

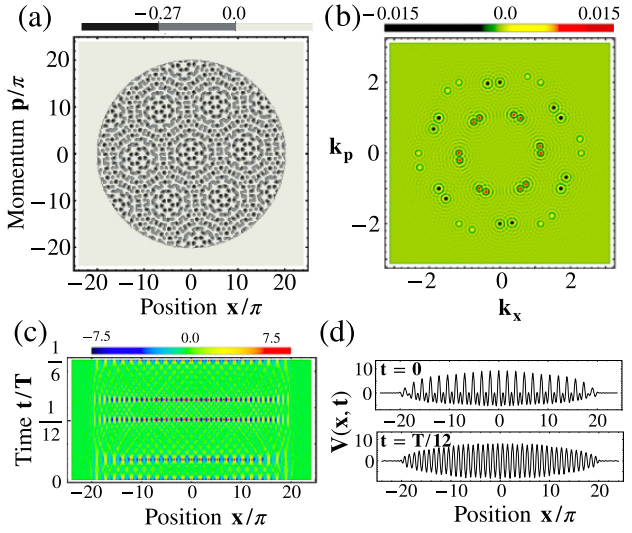

FIG. 3. Moiré superlattice in phase space. (a) Hamiltonian Q function of a Moiré superlattice with twisted angle $\theta = 10°$ and confined in a region with radius $R = 20\pi$. (b) Density plot of NcFT coefficient $\beta f_T(k_x, k_p)$. (c) Designed driving potential $V(x,t)$ for $t \in [0, T/6)$. (d) $V(x,t)$ at fixed time instants $t = 0$ (upper) and $t = T/12$ (lower).

superlattice is formed by overlaying two honeycomb lattices with a relative twist angle θ_0 in a finite region of radius R. Outside of this region $H_F^{(T)}(x,p) = 0$. The resulting Hamiltonian Q function for the twist angle $\theta_0 = 10°$ is shown in Fig. 3(a). As discussed above, overall the Floquet Hamiltonian should be smooth on the scale of the oscillator quantum fluctuations. As for the phase-space well example above, this can be implemented by applying a convolution with a Gaussian kernel to the initially discontinuous Floquet Hamiltonian. The ensuing transition between the Floquet lattice potential and the phase-space region with $H_F^{(T)}(x,p) = 0$ can be arbitrarily sharp compared to R or to the honeycomb lattice constant. A closed formula for the Floquet Hamiltonian is given in the SM Sec. VIII [57].

Applying our method, we calculate the NcFT coefficient $f_T(k_x, k_p)$ shown in Fig. 3(b). It is formed by three groups of twelve peaks. Each group of peaks is obtained from a single peak by applying one of the sixfold phase-space rotations and/or the rotation by the twist angle θ_0, cf Fig. 3(a). The width of all the peaks is $\propto R^{-1}$. All these features as well as the exact locations of the peaks can be read out from a closed-form solution for $f_T(k_x, k_p)$ given in the SM Sec. VIII [57]. In Fig. 3(c), we plot the ensuing driving potential $V(x,t)$ for $0 \le t < T_d$. [In this case, the driving period T_d is one-sixth of the natural period, $T_d = T/6$, reflecting the sixfold rotational-symmetry of our target Floquet Hamiltonian.] In Fig. 3(d), we also plot the instant driving potential at $t = 0$ and $t = T_d/2$ (or $t = T/12$). We note that the real-space driving potential is a sequence of discrete lattice potentials localized in a finite region of real space that are switched on for a short time interval. We note further that in the limit $R \to \infty$, the peaks in (k_x, k_p) space become δ functions, and the driving potential reduces to a discrete sequence of stroboscopic lattices with specific amplitudes, wavelengths, and phases [39,41,100,101]. Considering that the contact interaction of cold atoms turns into a long-distance Coulomb-like interaction in the rotating frame [39,41,58,101–106], many atoms in the phase space Moiré superlattice would mimic the behavior of electrons in twisted bilayer graphene [96–99].

Example IV: Artificial atomic spectrum.—Our method can be leveraged to implement a target spectrum $\{E_n\}$ as well as desired target eigenstates $\{|\psi_n\rangle\}$. As mentioned above, this could be useful for quantum simulations with interacting atoms. In this scenario, our method could be straightforwardly applied to the target Floquet Hamiltonian $\hat{H}_F^{(T)} = \sum_n E_n |\psi_n\rangle\langle\psi_n|$. For concreteness, we consider $|\psi_n\rangle = |n\rangle$ where $\{|n\rangle\}$ is the harmonic oscillator eigenbasis (Fock states). In this example, the Hamiltonian Q function and the NcFT coefficient can be easily expressed as a sum over the excitation number n,

$$H_Q^{(T)}(x,p) = e^{-\frac{x^2+p^2}{2\lambda}} \sum_{n=0}^{\infty} \frac{E_n}{n!} \left(\frac{x^2+p^2}{2\lambda}\right)^n, \qquad (11)$$

and

$$f_T(k_x, k_p) = \sum_{n=0}^{\infty} \lambda \frac{E_n}{\beta} e^{\lambda \frac{k^2}{4}} {}_1F_1\left(1+n; 1; -\lambda\frac{k^2}{2}\right), \qquad (12)$$

respectively. Here, ${}_1F_1(a;b;z)$ is the Kummer confluent hypergeometric function. The driving potential $V(x)$ can be straightforwardly calculated by plugging Eq. (12) into Eqs. (7) and (8). Note that since the NcFT coefficient $f_T(k\cos\tau, k\sin\tau)$ is independent of the angular coordinate τ, the driving potential $V(x)$ is *static*. This, in turn, follows from our choice of eigenbasis leading to a target Floquet Hamiltonian invariant under arbitrary phase-space rotations, cf. Eq. (11). Note further that the asymptotic behavior ${}_1F_1[1+n;1;-(k^2/2)] \sim [-(\lambda k^2/2n!)]^n e^{-(\lambda k^2/2)}$ for $k \to \infty$ ensures that the integral in Eq. (7) is well defined. In Fig. 4

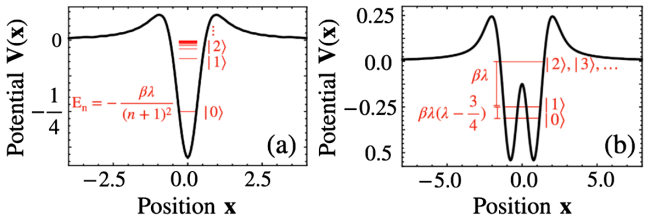

FIG. 4. Artificial spectrum: (a) designed hydrogen atomic levels with parameter $\lambda = \frac{1}{4}$; (b) levels $|0\rangle$ and $|1\rangle$ gapped from other degenerate levels with $\lambda = 1$. In both figures, the eigenstates $|n\rangle$ are the harmonic Fock states.

we display the potential $V(x)$ for two interesting choices of the spectrum $\{E_n\}$. In panel (a), we fix $\{E_n\}$ to be the spectrum of the hydrogen atom $E_n = -\beta\lambda/(n+1)^2$. In panel (b) we choose $E_1 = -\beta\lambda$ and $E_0 = E_1 - \beta\lambda(\lambda - \frac{3}{4})$ while all other levels are zero, $E_{n>1} = 0$. Thus, at $\lambda = 3/4$, the energies E_0 and E_1 of the second spectrum display an exact crossing.

State preparation.—Our method combined with an adiabatic ramp protocol following Ref. [31] can be exploited to prepare a desired quantum state. As an example, we demonstrate the preparation of a cat state in the ground state manifold of Hamiltonian Eq. (9), including also the effects of dissipation, see SM Sec. VI [57].

Experimental implementations.—In order to design arbitrary Hamiltonians in phase space, one needs the ability to engineer the driving real-space potential $V(x,t)$ in experiments. This might be difficult in practice. An alternative route is to directly use Eq. (7). In the SM Sec. VIB [57], we show that the target Floquet Hamiltonian can be well approximated by replacing the integral with the sum of a finite number of cosine lattice potentials. For example, we demonstrate the preparation of a three-legged cat state with 99% fidelity using only five such potentials. In cold atom experiments, the building block cosine lattice is formed by laser beams intersecting at an angle [41,59,60]. In experiments with superconducting circuits [61–63], a microwave cavity in series with a Josephson junction (JJ) biased by a dc voltage (V) is described by the Hamiltonian $\hat{\mathcal{H}}(t) = \hbar\omega_0\hat{a}^\dagger\hat{a} - E_J\cos[\omega_J t + \Delta(\hat{a}^\dagger + \hat{a})]$, where E_J is the JJ energy, $\omega_J = 2eV/\hbar$ is the Josephson frequency, and $\Delta = \sqrt{2e^2/(\hbar\omega_0 C)}$ with C the cavity capacitance [64–69,107–112].

Summary and outlook.—In this work, we have introduced a general constructive method to derive the driving potential, up to leading order in the Floquet-Magnus expansion, generating any arbitrary Floquet Hamiltonian of a single Bosonic mode. We have also shown that, in SM Secs. V and VI [57], it can be transferred to state-of-the-art experimental platforms to efficiently prepare quantum states as part of a long-lived quantum memory. A natural extension of our work would be to include higher-order perturbative corrections as the inverse problem of the Floquet-Magnus theory. Another exciting prospect is to extend our method to a many-body scenario by upgrading the single-particle plane-wave operator $\exp[i(k_x\hat{x} + k_p\hat{p})]$ used in Eq. (5) to a many-body equivalent $\exp[\sum_j i(k_x^j\hat{x}_j + k_p^j\hat{p}_j)]$. In experiments with superconducting circuits, this could be implemented coupling a dc-voltage biased JJ to multiple superconducting cavities [64–69].

We acknowledge helpful discussions with Florian Marquardt and Muxin Han.

*Corresponding author: lingzhen_guo@tju.edu.cn

[1] C. Gerry and P. Knight, Nonclassical light, in *Introductory Quantum Optics* (Cambridge University Press, Cambridge, England, 2004), pp. 150–194, ISBN: 9780521527354.
[2] D. V. Strekalov and G. Leuchs, *Nonlinear Interactions and Non-Classical Light* (Springer International Publishing, Cham, 2019), pp. 51–101, ISBN: 978-3-319-98402-5.
[3] B. Kubala, V. Gramich, and J. Ankerhold, Non-classical light from superconducting resonators coupled to voltage-biased Josephson junctions, Phys. Scr. T **165**, 014029 (2015).
[4] S. L. Braunstein and P. van Loock, Quantum information with continuous variables, Rev. Mod. Phys. **77**, 513 (2005).
[5] J.-W. Pan, Z.-B. Chen, C.-Y. Lu, H. Weinfurter, A. Zeilinger, and M. Żukowski, Multiphoton entanglement and interferometry, Rev. Mod. Phys. **84**, 777 (2012).
[6] Z.-H. Yan, J.-L. Qin, Z.-Z. Qin, X.-L. Su, X.-J. Jia, C.-D. Xie, and K.-C. Peng, Generation of non-classical states of light and their application in deterministic quantum teleportation, Fundam. Res. **1**, 43 (2021).
[7] Z. Leghtas, G. Kirchmair, B. Vlastakis, R. J. Schoelkopf, M. H. Devoret, and M. Mirrahimi, Hardware-efficient autonomous quantum memory protection, Phys. Rev. Lett. **111**, 120501 (2013).
[8] M. Mirrahimi, Z. Leghtas, V. V. Albert, S. Touzard, R. J. Schoelkopf, L. Jiang, and M. H. Devoret, Dynamically protected cat-qubits: a new paradigm for universal quantum computation, New J. Phys. **16**, 045014 (2014).
[9] R. W. Heeres, P. Reinhold, N. Ofek, L. Frunzio, L. Jiang, M. H. Devoret, and R. J. Schoelkopf, Implementing a universal gate set on a logical qubit encoded in an oscillator, Nat. Commun. **8**, 94 (2017).
[10] S. Rosenblum, P. Reinhold, M. Mirrahimi, L. Jiang, L. Frunzio, and R. J. Schoelkopf, Fault-tolerant detection of a quantum error, Science **361**, 266 (2018).
[11] C. Flühmann, T. L. Nguyen, M. Marinelli, V. Negnevitsky, K. Mehta, and J. P. Home, Encoding a qubit in a trapped-ion mechanical oscillator, Nature (London) **566**, 513 (2019).
[12] L. Hu, Y. Ma, W. Cai, X. Mu, Y. Xu, W. Wang, Y. Wu, H. Wang, Y. P. Song, C.-L. Zou *et al.*, Quantum error correction and universal gate set operation on a binomial bosonic logical qubit, Nat. Phys. **15**, 503 (2019).
[13] P. Campagne-Ibarcq, A. Eickbusch, S. Touzard, E. Zalys-Geller, N. E. Frattini, V. V. Sivak, P. Reinhold, S. Puri, S. Shankar, R. J. Schoelkopf *et al.*, Quantum error correction of a qubit encoded in grid states of an oscillator, Nature (London) **584**, 368 (2020).
[14] J. M. Gertler, B. Baker, J. Li, S. Shirol, J. Koch, and C. Wang, Protecting a bosonic qubit with autonomous quantum error correction, Nature (London) **590**, 243 (2021).
[15] P. T. Cochrane, G. J. Milburn, and W. J. Munro, Macroscopically distinct quantum-superposition states as a bosonic code for amplitude damping, Phys. Rev. A **59**, 2631 (1999).
[16] D. Gottesman, A. Kitaev, and J. Preskill, Encoding a qubit in an oscillator, Phys. Rev. A **64**, 012310 (2001).
[17] B. C. Travaglione and G. J. Milburn, Preparing encoded states in an oscillator, Phys. Rev. A **66**, 052322 (2002).

[18] M. H. Michael, M. Silveri, R. T. Brierley, V. V. Albert, J. Salmilehto, L. Jiang, and S. M. Girvin, New Class of Quantum Error-Correcting Codes for a Bosonic Mode, Phys. Rev. X **6**, 031006 (2016).

[19] V. V. Albert, K. Noh, K. Duivenvoorden, D. J. Young, R. T. Brierley, P. Reinhold, C. Vuillot, L. Li, C. Shen, S. M. Girvin *et al.*, Performance and structure of single-mode bosonic codes, Phys. Rev. A **97**, 032346 (2018).

[20] A. L. Grimsmo, J. Combes, and B. Q. Baragiola, Quantum Computing with Rotation-Symmetric Bosonic Codes, Phys. Rev. X **10**, 011058 (2020).

[21] I. Tzitrin, J. E. Bourassa, N. C. Menicucci, and K. K. Sabapathy, Progress towards practical qubit computation using approximate Gottesman-Kitaev-Preskill codes, Phys. Rev. A **101**, 032315 (2020).

[22] B. M. Terhal, J. Conrad, and C. Vuillot, Towards scalable bosonic quantum error correction, Quantum Sci. Technol. **5**, 043001 (2020).

[23] A. Joshi, K. Noh, and Y. Y. Gao, Quantum information processing with bosonic qubits in circuit QED, Quantum Sci. Technol. **6**, 033001 (2021).

[24] W. Cai, Y. Ma, W. Wang, C.-L. Zou, and L. Sun, Bosonic quantum error correction codes in superconducting quantum circuits, Fundam. Res. **1**, 50 (2021).

[25] S. Krastanov, V. V. Albert, C. Shen, C.-L. Zou, R. W. Heeres, B. Vlastakis, R. J. Schoelkopf, and L. Jiang, Universal control of an oscillator with dispersive coupling to a qubit, Phys. Rev. A **92**, 040303(R) (2015).

[26] T. Fösel, S. Krastanov, F. Marquardt, and L. Jiang, Efficient cavity control with snap gates, arXiv:2004.14256.

[27] M. Kudra, M. Kervinen, I. Strandberg, S. Ahmed, M. Scigliuzzo *et al.*, Robust preparation of Wigner-negative states with optimized snap-displacement sequences, PRX Quantum **3**, 030301 (2022).

[28] S. Puri, A. Grimm, P. Campagne-Ibarcq, A. Eickbusch, K. Noh, G. Roberts, L. Jiang, M. Mirrahimi, M. H. Devoret, and S. M. Girvin, Stabilized Cat in a Driven Non-Linear Cavity: A Fault-Tolerant Error Syndrome Detector, Phys. Rev. X **9**, 041009 (2019).

[29] M. Rymarz, S. Bosco, A. Ciani, and D. P. DiVincenzo, Hardware-Encoding Grid States in a Nonreciprocal Superconducting Circuit, Phys. Rev. X **11**, 011032 (2021).

[30] J. Conrad, Twirling and Hamiltonian engineering via dynamical decoupling for Gottesman-Kitaev-Preskill quantum computing, Phys. Rev. A **103**, 022404 (2021).

[31] X. C. Kolesnikow, R. W. Bomantara, A. C. Doherty, and A. L. Grimsmo, Gottesman-Kitaev-Preskill state preparation using periodic driving, arXiv:2303.03541.

[32] G. M. Zaslavskii, M. Y. Zakharov, R. Z. Sagdeev, D. Usikov, and A. A. Chernikov, Stochastic web and diffusion of particles in a magnetic field, Zh. Eksp. Teor. Fiz. **91**, 500 (1986), http://jetp.ras.ru/cgi-bin/dn/e_064_02_0294.pdf.

[33] G. P. Berman, V. Y. Rubaev, and G. M. Zaslavsky, The problem of quantum chaos in a kicked harmonic oscillator, Nonlinearity **4**, 543 (1991).

[34] P. Leboeuf, J. Kurchan, M. Feingold, and D. P. Arovas, Phase-space localization: Topological aspects of quantum chaos, Phys. Rev. Lett. **65**, 3076 (1990).

[35] P. Leboeuf, J. Kurchan, M. Feingold, and D. P. Arovas, Topological aspects of quantum chaos, Chaos **2**, 125 (1992).

[36] T. P. Billam and S. A. Gardiner, Quantum resonances in an atom-optical δ-kicked harmonic oscillator, Phys. Rev. A **80**, 023414 (2009).

[37] L. Guo, M. Marthaler, and G. Schön, Phase space crystals: A new way to create a quasienergy band structure, Phys. Rev. Lett. **111**, 205303 (2013).

[38] Y. Zhang, J. Gosner, S. M. Girvin, J. Ankerhold, and M. I. Dykman, Time-translation-symmetry breaking in a driven oscillator: From the quantum coherent to the incoherent regime, Phys. Rev. A **96**, 052124 (2017).

[39] P. Liang, M. Marthaler, and L. Guo, Floquet many- body engineering: Topology and many-body physics in phase space lattices, New J. Phys. **20**, 023043 (2018).

[40] N. Lörch, Y. Zhang, C. Bruder, and M. I. Dykman, Quantum state preparation for coupled period tripling oscillators, Phys. Rev. Res. **1**, 023023 (2019).

[41] L. Guo, V. Peano, and F. Marquardt, Phase space crystal vibrations: Chiral edge states with preserved time- reversal symmetry, Phys. Rev. B **105**, 094301 (2022).

[42] A. Eckardt and E. Anisimovas, High-frequency approximation for periodically driven quantum systems from a Floquet-space perspective, New J. Phys. **17**, 093039 (2015).

[43] M. Bukov, L. D'Alessio, and A. Polkovnikov, Universal high-frequency behavior of periodically driven systems: from dynamical stabilization to Floquet engineering, Adv. Phys. **64**, 139 (2015).

[44] A. Eckardt, Colloquium: Atomic quantum gases in periodically driven optical lattices, Rev. Mod. Phys. **89**, 011004 (2017).

[45] S. Rahav, I. Gilary, and S. Fishman, Effective Hamiltonians for periodically driven systems, Phys. Rev. A **68**, 013820 (2003).

[46] N. Goldman and J. Dalibard, Periodically Driven Quantum Systems: Effective Hamiltonians and Engineered Gauge Fields, Phys. Rev. X **4**, 031027 (2014).

[47] F. Casas, J. A. Oteo, and J. Ros, Floquet theory: Exponential perturbative treatment, J. Phys. A **34**, 3379 (2001).

[48] S. Blanes, F. Casas, J. Oteo, and J. Ros, The Magnus expansion and some of its applications, Phys. Rep. **470**, 151 (2009).

[49] T. Mikami, S. Kitamura, K. Yasuda, N. Tsuji, T. Oka, and H. Aoki, Brillouin-Wigner theory for high-frequency expansion in periodically driven systems: Application to Floquet topological insulators, Phys. Rev. B **93**, 144307 (2016).

[50] M. S. Rudner and N. H. Lindner, Band structure engineering and non-equilibrium dynamics in Floquet topological insulators, Nat. Rev. Phys. **2**, 229 (2020).

[51] M. Jangjan and M. V. Hosseini, Floquet engineering of topological metal states and hybridization of edge states with bulk states in dimerized two-leg ladders, Sci. Rep. **10**, 14256 (2020).

[52] M. Jangjan, L. E. F. Foa Torres, and M. V. Hosseini, Floquet topological phase transitions in a periodically quenched dimer, Phys. Rev. B **106**, 224306 (2022).

[53] M. Marthaler and M. I. Dykman, Switching via quantum activation: A parametrically modulated oscillator, Phys. Rev. A **73**, 042108 (2006).

[54] V. Peano, M. Marthaler, and M. I. Dykman, Sharp tunneling peaks in a parametric oscillator: Quantum resonances missing in the rotating wave approximation, Phys. Rev. Lett. **109**, 090401 (2012).

[55] L. Guo, V. Peano, M. Marthaler, and M. I. Dykman, Quantum critical temperature of a modulated oscillator, Phys. Rev. A **87**, 062117 (2013).

[56] M. Scully and M. Zubairy, Quantum critical temperature of a modulated oscillator, in *Quantum Optics* (Cambridge University Press, Cambridge, England, 1997), ISBN: 9780521435956.

[57] See Supplemental Material at http://link.aps.org/supplemental/10.1103/PhysRevLett.132.023602 for details, which includes Refs. [7,8,13,16,18,20,22,27–31,37,41,48,49,54,59–94].

[58] L. Guo and P. Liang, Condensed matter physics in time crystals, New J. Phys. **22**, 075003 (2020).

[59] H. Moritz, T. Stöferle, M. Köhl, and T. Esslinger, Exciting collective oscillations in a trapped 1d gas, Phys. Rev. Lett. **91**, 250402 (2003).

[60] Z. Hadzibabic, S. Stock, B. Battelier, V. Bretin, and J. Dalibard, Interference of an array of independent Bose-Einstein condensates, Phys. Rev. Lett. **93**, 180403 (2004).

[61] F. Chen, J. Li, A. D. Armour, E. Brahimi, J. Stettenheim, A. J. Sirois, R. W. Simmonds, M. P. Blencowe, and A. J. Rimberg, Realization of a single-Cooper-pair Josephson laser, Phys. Rev. B **90**, 020506(R) (2014).

[62] M. Hofheinz, F. Portier, Q. Baudouin, P. Joyez, D. Vion, P. Bertet, P. Roche, and D. Esteve, Bright side of the coulomb blockade, Phys. Rev. Lett. **106**, 217005 (2011).

[63] F. Chen, A. J. Sirois, R. W. Simmonds, and A. J. Rimberg, Introduction of a dc bias into a high-Q superconducting microwave cavity, Appl. Phys. Lett. **98**, 132509 (2011).

[64] A. D. Armour, M. P. Blencowe, E. Brahimi, and A. J. Rimberg, Universal quantum fluctuations of a cavity mode driven by a Josephson junction, Phys. Rev. Lett. **111**, 247001 (2013).

[65] A. D. Armour, B. Kubala, and J. Ankerhold, Josephson photonics with a two-mode superconducting circuit, Phys. Rev. B **91**, 184508 (2015).

[66] M. Trif and P. Simon, Photon cross-correlations emitted by a Josephson junction in two microwave cavities, Phys. Rev. B **92**, 014503 (2015).

[67] P. P. Hofer, J.-R. Souquet, and A. A. Clerk, Quantum heat engine based on photon-assisted Cooper pair tunneling, Phys. Rev. B **93**, 041418(R) (2016).

[68] S. Dambach, B. Kubala, and J. Ankerhold, Generating entangled quantum microwaves in a Josephson-photonics device, New J. Phys. **19**, 023027 (2017).

[69] B. Lang, G. F. Morley, and A. D. Armour, Discrete time translation symmetry breaking in a Josephson junction laser, Phys. Rev. B **107**, 144509 (2022).

[70] L. Guo and M. Marthaler, Synthesizing lattice structures in phase space, New J. Phys. **18**, 023006 (2016).

[71] W. H. Louisell, *Quantum Statistical Properties of Radiation* (Wiley, New York, 1973).

[72] L. Gilles, B. M. Garraway, and P. L. Knight, Generation of nonclassical light by dissipative two-photon processes, Phys. Rev. A **49**, 2785 (1994).

[73] M. I. Dykman, Critical exponents in metastable decay via quantum activation, Phys. Rev. E **75**, 011101 (2007).

[74] S. Puri, L. St-Jean, J. A. Gross, A. Grimm, N. E. Frattini, P. S. Iyer, A. Krishna, S. Touzard, L. Jiang, A. Blais *et al.*, Bias-preserving gates with stabilized cat qubits, Sci. Adv. **6**, eaay5901 (2020).

[75] M. I. Dykman, M. Marthaler, and V. Peano, Quantum heating of a parametrically modulated oscillator: Spectral signatures, Phys. Rev. A **83**, 052115 (2011).

[76] M. A. Nielsen and I. L. Chuang, *Quantum Computation and Quantum Information: 10th Anniversary Edition* (Cambridge University Press, Cambridge, England, 2010).

[77] S. Rosenblum, P. Reinhold, M. Mirrahimi, L. Jiang, L. Frunzio, and R. J. Schoelkopf, Fault-tolerant detection of a quantum error, Science **361**, 266 (2018).

[78] D. F. V. James, P. G. Kwiat, W. J. Munro, and A. G. White, Measurement of qubits, Phys. Rev. A **64**, 052312 (2001).

[79] A. Eickbusch, V. Sivak, A. Z. Ding, S. S. Elder, S. R. Jha, J. Venkatraman, B. Royer, S. M. Girvin, R. J. Schoelkopf, and M. H. Devoret, Fast universal control of an oscillator with weak dispersive coupling to a qubit, Nat. Phys. **18**, 1464 (2022).

[80] V. V. Sivak, A. Eickbusch, B. Royer, S. Singh, I. Tsioutsios, S. Ganjam, A. Miano, B. L. Brock, A. Z. Ding, L. Frunzio *et al.*, Real-time quantum error correction beyond break-even, Nature (London) **616**, 50 (2023).

[81] N. Bergeal, R. Vijay, V. E. Manucharyan, I. Siddiqi, R. J. Schoelkopf, S. M. Girvin, and M. H. Devoret, Analog information processing at the quantum limit with a Josephson ring modulator, Nat. Phys. **6**, 296 (2010).

[82] N. Roch, E. Flurin, F. Nguyen, P. Morfin, P. Campagne-Ibarcq, M. H. Devoret, and B. Huard, Widely tunable, nondegenerate three-Wave mixing microwave device operating near the quantum limit, Phys. Rev. Lett. **108**, 147701 (2012).

[83] J. Kelly *et al.*, State preservation by repetitive error detection in a superconducting quantum circuit, Nature (London) **519**, 66 (2015).

[84] F. Arute *et al.*, Quantum supremacy using a programmable superconducting processor, Nature (London) **574**, 505 (2019).

[85] Y. Kim, A. Eddins, S. Anand, K. X. Wei, E. van den Berg, S. Rosenblatt, H. Nayfeh, Y. Wu, M. Zaletel, K. Temme *et al.*, Evidence for the utility of quantum computing before fault tolerance, Nature (London) **618**, 500 (2023).

[86] S. Lloyd, Universal quantum simulators, Science **273**, 1073 (1996).

[87] L. Guo (to be published).

[88] K. Jacobs, Wave-function Monte Carlo method for simulating conditional master equations, Phys. Rev. A **81**, 042106 (2010).

[89] H. M. Wiseman and G. J. Milburn, *Quantum Measurement and Control* (Cambridge University Press, Cambridge, England, 2009), ISBN: 9780521804424.

[90] N. Ofek, A. Petrenko, R. Heeres, P. Reinhold, Z. Leghtas, B. Vlastakis, Y. Liu, L. Frunzio, S. M. Girvin, L. Jiang *et al.*, Extending the lifetime of a quantum bit with error correction in superconducting circuits, Nature (London) **536**, 441 (2016).
[91] R. N. Bracewell, Strip integration in radio astronomy, Aust. J. Phys. **9**, 198 (1956).
[92] R. Ng, Fourier slice photography, ACM Trans. Graph. **24**, 735 (2005).
[93] G. B. Arfken and H. J. Weber, *Mathematical Methods for Physicists*, 6th ed. (Academic Press, New York, 2005), ISBN: 978-0120598762.
[94] M. Dykman, *Fluctuating Nonlinear Oscillators: From Nanomechanics to Quantum Superconducting Circuits* (Oxford University Press, New York, 2012), ISBN: 9780199691388.
[95] A. Bachtold, J. Moser, and M. I. Dykman, Mesoscopic physics of nanomechanical systems, Rev. Mod. Phys. **94**, 045005 (2022).
[96] R. Bistritzer and A. H. MacDonald, Moire bands in twisted double-layer graphene, Proc. Natl. Acad. Sci. U.S.A. **108**, 12233 (2011).
[97] Y. Cao, V. Fatemi, A. Demir, S. Fang, S. L. Tomarken, J. Y. Luo, J. D. Sanchez-Yamagishi, K. Watanabe, T. Taniguchi, E. Kaxiras *et al.*, Correlated insulator behaviour at half-filling in magic-angle graphene superlattices, Nature (London) **556**, 80 (2018).
[98] Y. Cao, V. Fatemi, S. Fang, K. Watanabe, T. Taniguchi, E. Kaxiras, and P. Jarillo-Herrero, Unconventional superconductivity in magic-angle graphene superlattices, Nature (London) **556**, 43 (2018).
[99] A. Thomson, S. Chatterjee, S. Sachdev, and M. S. Scheurer, Triangular antiferromagnetism on the honeycomb lattice of twisted bilayer graphene, Phys. Rev. B **98**, 075109 (2018).
[100] L. Guo, M. Liu, and M. Marthaler, Effective long-distance interaction from short-distance interaction in a periodically driven one-dimensional classical system, Phys. Rev. A **93**, 053616 (2016).
[101] L. Guo, Many-body physics in phase space, in *Phase Space Crystals* (IOP Publishing, Bristol, UK, 2021), pp. 4–1 to 4–28, ISBN: 978-0-7503-3563-8.
[102] K. Sacha, Anderson localization and Mott insulator phase in the time domain, Sci. Rep. **5**, 10787 (2015).
[103] M. Mierzejewski, K. Giergiel, and K. Sacha, Many-body localization caused by temporal disorder, Phys. Rev. B **96**, 140201(R) (2017).
[104] K. Giergiel, A. Miroszewski, and K. Sacha, Time crystal platform: From quasicrystal structures in time to systems with exotic interactions, Phys. Rev. Lett. **120**, 140401 (2018).
[105] K. Sacha, *Condensed Matter Physics in the Time Dimension* (Springer International Publishing, Cham, 2020), pp. 173–235, ISBN: 978-3-030-52523-1.
[106] P. Hannaford and K. Sacha, Condensed matter physics in big discrete time crystals, AAPPS Bull. **32**, 12 (2022).
[107] V. Gramich, B. Kubala, S. Rohrer, and J. Ankerhold, From Coulomb-blockade to nonlinear quantum dynamics in a superconducting circuit with a resonator, Phys. Rev. Lett. **111**, 247002 (2013).
[108] J. Leppäkangas, G. Johansson, M. Marthaler, and M. Fogelström, Nonclassical photon pair production in a voltage-biased Josephson junction, Phys. Rev. Lett. **110**, 267004 (2013).
[109] J. Leppäkangas, M. Fogelström, A. Grimm, M. Hofheinz, M. Marthaler, and G. Johansson, Antibunched photons from inelastic Cooper-pair tunneling, Phys. Rev. Lett. **115**, 027004 (2015).
[110] J. Leppäkangas, M. Fogelström, M. Marthaler, and G. Johansson, Correlated cooper pair transport and microwave photon emission in the dynamical Coulomb blockade, Phys. Rev. B **93**, 014506 (2016).
[111] B. Kubala, V. Gramich, and J. Ankerhold, Non-classical light from superconducting resonators coupled to voltage-biased Josephson junctions, Phys. Scr. T **165**, 014029 (2015).
[112] B. Lang and A. D. Armour, Multi-photon resonances in Josephson junction-cavity circuits, New J. Phys. **23**, 033021 (2021).
[113] H. Srivastava and J. Choi, in *Zeta and q-Zeta Functions and Associated Series and Integrals*, edited by H. Srivastava and J. Choi (Elsevier, London, 2012), pp. 1–140, ISBN: 978-0-12-385218-2.